Faculty of Electrical Engineering
Department of Radioelectronics

Bachelor's thesis

Flight Computer for Small Rocket

Aleš Zapadlo

Bachelor's Programme:
Electronics and Communication (BP77)

Supervisor:
Doc. Ing. Stanislav Vítek, PhD.

Prague, May 2023

BACHELOR‘S THESIS ASSIGNMENT

I. Personal and study details

Student's name: **Zapadlo Aleš** Personal ID number: **491935**

Faculty / Institute: **Faculty of Electrical Engineering**

Department / Institute: **Department of Radioelectronics**

Study program: **Electronics and Communications**

II. Bachelor’s thesis details

Bachelor’s thesis title in English:

Flight Computer for Small Rocket

Bachelor’s thesis title in Czech:

Letový počítač pro malou raketu

Guidelines:

The work aims to design and implement a flight computer for a small rocket. Follow the following instructions:
* The computer is based on the STM32 microcontroller
* Sensors are connected to the computer (at least a barometer and an accelerometer, optionally others), and data from the sensors are logged to a suitable storage medium
* The computer is battery-powered, with a separate power supply able to cut the nylon fiber

Bibliography / sources:

[1] NOVIELLO, Carmine Mastering STM32, 2018, Leanpub
[2] SKŘIVÁNEK, Vojtěch Programujeme STM32 - bez knihoven, 2022, TZ-one

Name and workplace of bachelor’s thesis supervisor:

doc. Ing. Stanislav Vítek, Ph.D. Department of Radioelectronics FEE

Name and workplace of second bachelor’s thesis supervisor or consultant:

Date of bachelor’s thesis assignment: **30.01.2023** Deadline for bachelor thesis submission: _____

Assignment valid until: **22.09.2024**

doc. Ing. Stanislav Vítek, Ph.D. Supervisor’s signature	doc. Ing. Stanislav Vítek, Ph.D. Head of department’s signature	prof. Mgr. Petr Páta, Ph.D. Dean’s signature

III. Assignment receipt

The student acknowledges that the bachelor’s thesis is an individual work. The student must produce his thesis without the assistance of others, with the exception of provided consultations. Within the bachelor’s thesis, the author must state the names of consultants and include a list of references.

. _____
Date of assignment receipt

_____
Student’s signature

ABSTRACT

This paper presents the design process and realization of a flight computer developed for a small rocket competing in the 2023 *Czech Rocket Challenge*. The flight computer was required to meet a variety of requirements relating to electronics, mechanics, and redundancy. To achieve these requirements, the flight computer employed an STM32 processor with a built-in LoRa radio for communication. The board also included a 70 F supercapacitor as an alternative power source and a power selector that switches between the battery and the supercapacitor. The design of the flight computer was validated by a stratospheric flight on a weather balloon.

KEYWORDS

Rocket, Flight Computer, LoRa 868MHz, Supercapacitor, SEPIC, Stratosphere, Weather Balloon, Ideal Diode, Power selector

ABSTRAKT

Tato práce představuje proces návrhu a realizace letového počítače vyvinutého pro malou raketu soutěžící v roce 2023 v soutěži *Czech Rocket Challenge*. Letový počítač musel splňovat různé požadavky vztahující se k elektronice, mechanice a redundanci. Pro dosažení tohoto cíle byl použit procesor STM32 s integrovaným rádiem LoRa pro komunikaci. Deska zahrnuje superkondenzátor jako záložní zdroj energie a selektor napájení mezi baterií a superkondenzátorem. Návrh letového počítače byl ověřen letem na meteorologickém balónu do stratosféry.

KLÍČOVÁ SLOVA

Raketa, Letový počítač, LoRa 868MHz, Superkondenzátor, SEPIC, Stratosféra, Balón, Ideální dioda, Selektor napájení

ACKNOWLEDGEMENT

First and foremost, I would like to express my gratitude to my thesis advisor, doc. Ing. Stanislav Vítek, Ph.D. Under his excellent and professional guidance I could explore my every idea, while recieving valuable feedback.

I would also like to express my thanks to the whole CTU Space Research club, especially to Lukáš Mičan. Another notable mention is my own father, Petr Zapadlo. They provided me with the necessary know-how for the project to work, as well as technical equipment for its realization.

Last but not least, I would like to acknowledge the support from my family and friends. Your generosity, patience and kindness helped me to reach this important milestone in my academic career.

DECLARATION

I declare that the presented work was developed independently and that I have listed all sources of information used within it in accordance with the methodical instructions for observing the ethical principles in the preparation of university theses.

HOW TO CITE

ZAPADLO, Aleš. *Flight Computer for Small Rocket*: bachelor's thesis. Prague: Czech Technical University in Prague, Faculty of Electrical Engineering, Department of Radioelectronics, 2023. 37 p. Supervised by Doc. Ing. Stanislav Vítek, PhD.

Contents

List of Figures

List of Acronyms

ADC ..... Analog to Digital Converter
CHMI ..... Czech HydroMeteorological Institute
CRC ..... Czech Rocket Challenge
EEPROM ..... Electrically Erasable Programmable Read-Only Memory
EM ..... Electro-Magnetic
FC ..... Flight Computer
FTDI ..... Future Technology Devices International limited
GPIO ..... General-Purpose Input/Output
I2C ..... Inter-Integrated Circuit
IC ..... Integrated Circuit
LGA ..... Land Grid Array
LoRa ..... Long Range
LoRaWAN ..... Long Range Wide Area Network
MCU ..... Microcontroller Unit
MEMS ..... Micro-ElectroMechanical System
MOSFET ..... Metal-Oxide-Semiconductor Field-Effect Transistor
MPA ..... Microstrip Patch Antenna
MSOP ..... Mini Small Outline Package
PCB ..... Printed Circuit Board
PWM ..... Pulse Width Modulation
QFN ..... Quad-Flat No-leads package
QFP ..... Quad-Flat Package
RF ..... Radio Frequency
SEPIC ..... Single-Ended Primary-Inductance Converter
SMD ..... Surface Mount Device
SNR ..... Singal-to-Noise Ratio
SPI ..... Serial Peripheral Interface
STM32 ..... An MCU from STmicroelectronics
SuperC ..... Super Capacitor
SWD ..... Serial Wire Debug
THT ..... Through Hole Technology
UART ..... Universal Asynchronous Receiver/Transmitter
USART ..... Universal Synchronous/Asynchronous Receiver/Transmitter

1 Introduction

In recent years, there has been a resurgence of interest in rocket technology, which is often referred to as the "Second Space Age". This renewed interest is being driven by the emergence of private launch providers such as SpaceX and Blue Origin, who are challenging the traditional government organizations (NASA, ESA) in the space race.

In this context, the work presented aims to address some of the challenges faced by professional space engineers, albeit in a more easy manner. Specifically, the objective is to design a flight computer that is both small and lightweight, yet capable of meeting all critical requirements for a small ($\sim$40 cm in length) rocket that will participate in the Czech Rocket Challenge (CRC).

The research builds on the experience and previous work of the CTU Space Research club, which has already designed and tested a flight computer for a previous rocket. However, the current work represents a significant improvement, as the board has been miniaturized while retaining key functionality. In addition, a backup power source for the logical part has been included, and the flight computer has the capability of serving as a backup computer for a second rocket.

First, a detailed description of all the requirements for the flight computer will be presented. Then, the design section will explain the solutions to the problems that arose from the requirements. Finally, the realization section will present the consideration that went into the board design, the board assembly, power sources measurements and at last, validation of the design by a flight of the computer on a weather balloon.

2 Requirements

Flight computer (FC) is a critical part of the rocket, as critical as the engine itself. Any failure, power loss or unintended behavior of the computer might cause safety concerns during launch or loss of the rocket in the worst scenario. For that reason, the FC's key functions must be as redundant as possible. It is crucial to expect that some parts of the system might not work, either by design or an accident. Therefore, the system should include failsafes or ways to simplify ad-hoc solutions to unexpected problems. The flight computer ground operators must be able to solve possible problems that might arise during the development of the whole rocket by multiple means, even if they were not primarily designed for the function. The design requirements for the flight computer were based on the rules of the CRC, as well as experience from previous competitions.

2.1 Physical requirements

Regarding the physical dimensions of the rocket[1], approximate size of the rocket from last year's competition was used. The dimensions can be seen in Figure 2.1. Even though the size of the new rocket will probably change, the most critical dimension, the width of the hull, will likely stay the same.

The hull width determines both the maximum width of the FC (in this case 3.5 cm) and the radius which dictates the maximum height of the components, including their distribution. The length of the FC is not limited, but the parachute must fit into the tubular fuselage, which significantly limits available vertical space.

The rules do not limit the maximum weight of the flight computer. However, by having the FC very light, we can achieve the maximum altitude, which is one of the goals of the competition.

2.2 Mechanical requirements

As stated in the physical requirements section, weight plays a critical role. Another important aspect of weight is its distribution – during high-G ascend (it is reasonable to expect up to 10 Gs), every bit of mass dissymmetry affects the craft much more. Lastly, the FC components must survive the acceleration and deceleration during the launch and the subsequent landing, respectively.

[1] Drawing was created in OnShape program

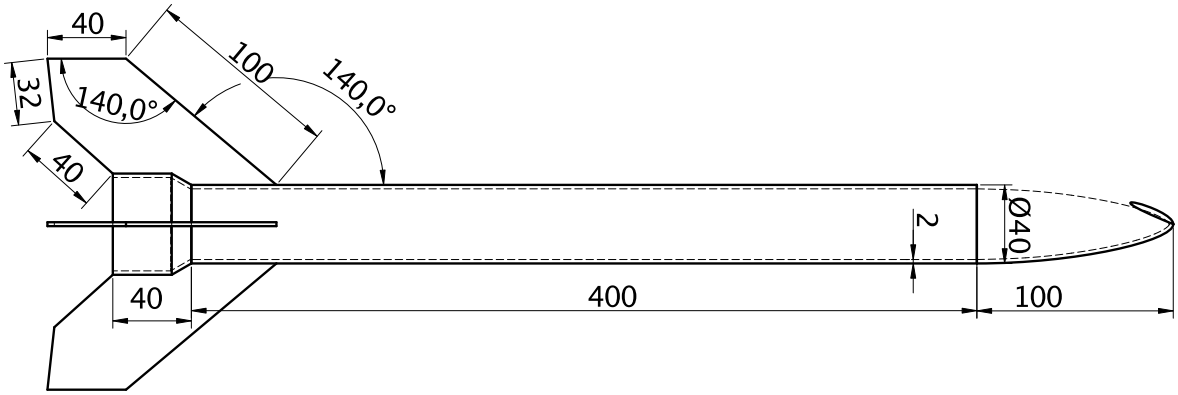

Fig. 2.1: Simplified blueprint of the rocket; dimensions in mm, degrees

2.3 Electrical requirements

The flight computer has two key functions – detection of the apogee[2] and subsequent parachute deployment.

A standard method to deploy a parachute is to cut a nylon string with a heated wire. When the tension held by the string is released, a spring mechanism will deploy the parachute. Another common but more sophisticated deployment system uses a servomotor to unlock a pre-tensioned deployment mechanism.

The rocket this FC is planned for uses the nylon cutting method – because the heating element needs to achieve high temperature, the flight computer must be able to supply it with high enough current.

One of the important things to note is that the FC should be able to serve as a backup flight computer for CTU Space Research's main rocket, *Illustria*. However, since *Illustria* uses the servomotor deployment system, it is preferable for FC to have the ability control servos as well.

The implication of having to power a servo motor is the need to implement a 5 V power source, which will provide enough power for the servo to operate. Moreover, *Illustria* uses up to a 4-cell Li-Po battery pack, so the FC must be able to handle at least 14.8 V. However, having a 4-cell battery is unnecessary for the small rocket, for which 1-cell LiPo at 3.8 V is enough. From these requirements, it implies that the FC must operate at voltages ranging from 3.8 V to 14.8 V.

Also, the FC must contain a second power source in case the main battery gets damaged, disconnected, or any other problem arises. Since not deploying a parachute means losing the competition, the rocket, and all the data, it is a crucial feature that must be implement into the FC.

[2]highest point in flight trajectory

Moreover, the CRC rules state that the rocket must be able to remain powered on the launch ramp for at least 30 minutes and then perform launch with successful vehicle recovery. Depending on the environment, the whole launch sequence can span around 1h and 30 minutes – up to 30 minutes of stand-by on the ramp required by the CRC, 5 minutes of flight, and one hour of search for the rocket in a high corn field in the worst case scenario. Because the exact consumption of the flight computer is not known at the time of design, the calculation of the required battery size shall be done once the flight computer is finished and consumption measured.

2.4 Sensors requirements

Required sensors for the rocket to operate correctly:

- Pressure sensor to determine reached hight
- Acceleration and gyroscope sensor for detecting the trajectory apogee for parachute deployment

Optional sensors to provide additional data:

- Temperature sensor
- Magnetic sensor

2.5 Wireless communication requirements

Having a wireless connection to a ground station is not strictly required, but the option to communicate with the rocket before the launch and during the flight would provide better control over the rocket.

Should such system be implemented, bidirectional communication is preferable. Not all launches go according to the plan, and having the means to manually trigger the abort sequence would make the rocket safer and minimize possible damage to the rocket itself. The Czech Republic legislation allows multiple frequency bands to be used without a licence [1]. However, only two of them are in widespread use – 433 MHz and 868 MHz bands. Since the maximum effective radiated power on the 868 MHz band is higher than on the 433 MHz band, it is the preferred choice.

2.6 Requirements summary

All the requirement mentioned above can be summarized into desired attributes of the flight computer:

- Physical dimensions with width < 3.5 cm, length as short as possible, no high components on side edges of the PCB

- As symmetrical as possible, no tall and heavy components, no components with moving parts other than MEMS
- High-current source for nylon cutting parachute deployment
- 5 V power source for servo parachute deployment
- Input voltage in the range of at least 3.8 V - 14.8 V
- Backup power source in case the main battery fails; FC must be able to perform mission-critical functions being powered by the backup alone
- At least 30 minutes of powered-on standby time with subsequent launch
- Accelerometer, gyroscope, and pressure sensors are required; magnetic and temperature sensors are optional
- Optional: 868 MHz radio with bidirectional communication allowing for manually triggering abort sequence

3 Design

3.1 Electric design decisions

To achieve the desired attributes of the FC, solutions for each necessary feature needed to be identified. The backup power source is the most critical component, and its weight should be minimized since it will only be utilized in case of an failure. Furthermore, it should be low maintenance because it will be tightly connected to the flight computer and cannot be frequently maintained. Scalability is essential to experimentally determine the ideal backup time (=capacity) to weight ratio. Finally, the backup power source must be able to deliver the high currents required to cut the nylon string. After evaluating these factors, a supercapacitor (SuperC) was chosen as the best compromise. It is lighter than batteries (although slightly larger in volume), can be discharged to 0 V without negative consequences, and can provide the necessary high current. However, the major drawback of a SuperC is its low voltage, which peaks at around 3 V. Voltage this low increases the complexity of the board, since the electronics runs at 3.3 V, necessitating two power supplies – a step-down from V_{IN} to V_{SuperC} and a step-up from V_{SuperC} to 3.3 V, which powers all integrated circuits and the MCU.

Theoretical energy capacity of a capacitor can be calculated with an equation:

$$E_J = \frac{1}{2} \cdot C \cdot V^2 \quad [\text{J}] \tag{3.1}$$

$$E = E_J \frac{1000}{60 * 60} \quad [\text{mAh}] \tag{3.2}$$

By combining the two previous equations, energy of a capacitor in mAh can be calculated, which allows for easy comparison with batteries.

$$E = \frac{1}{7.2} \cdot C \cdot V^2 \quad [\text{mAh}] \tag{3.3}$$

Using Equation (3.3), a 70 F SuperC with maximum voltage of 3 V has total energy capacity of 87.5 mAh. Even considering only 50% of the energy to be recoverable, this capacity is more than sufficient to power the system for a significant amount of time.

Moving on to the 5 V supply, it must be designed to power a servomotor or any other external module. Despite servomotors generally not requiring an excessive amount of power to run (< 1 A), the servomotors used in *Illustria* can consume up to multiple amps during initial acceleration of the arm. Thus, the 5 V power supply must provide at least 1 A of continuous current and have enough capacity to cover the current peaks.

However, connecting the 5 V supply to the SuperC would significantly increase the current requirements of the 3 V power supply and introduce another power loss. Therefore, the only viable solution is to connect the 5 V power supply to the main battery, voltage of which can span the whole 3.8V-14.8 V range. This range can be lower and higher than the output voltage, presenting a problem. To address this issue, the single-ended primary-inductance converter (SEPIC) was chosen, which can increase as well as decrease the input voltage to constant output voltage. Additionally, the power supply should have the option to be turned off since it will not be necessary unless a servomotor or another module is utilized.

Designing power supplies for a project such as this one requires great attention to detail, as switched currents may generate unwanted noise in nearby sensors and electronics due to necessary dimensional proximity.

Next, let's consider the requirements for cutting the nylon string with a hot wire. Since the resistive wire behaves almost like a short circuit when burning the nylon string, the switching transistor must have a low voltage drop to avoid unnecessary power loss and thermal issues.

Lastly, the power delivery system must be carefully designed to ensure that the FC can perform mission-critical functions even when the battery is not available or damaged. This requires a way to switch between power sources (battery and SuperC) to power the nylon cutting wire, as well as the 5 V SEPIC. The switching element must meet challenging requirements due to the properties of the power delivery system:

- it must have a little to no voltage drop; otherwise, the SuperC will not be able to provide enough current for the wire to warm up adequately to burn the nylon string
- it must prevent reverse current – the current from high voltage battery must not flow into the 3 V SuperC, as well as should the battery be short-circuited, the SuperC must not be discharged by the short circuit

These requirements rule out using a regular diode or even a low-drop Schottky, as the expected voltage drop of >0.5 V would significantly limit the maximum power that can be delivered from the SuperC, even when fully charged. Moreover, since the diode would always be "in the way of the current", the voltage drop would substantially impact the system's efficiency and reduce the maximum extractable power from the capacitor. These inefficiencies would need to be compensated by carrying a larger battery, increasing the computer's weight.

Fortunately, a colleague provided a solution to the challenge – the "ideal diode" circuit. This circuit involves using a MOSFET in the reverse configuration and a controller in the form of an IC. The controller detects the flow of current through the substrate diode, and once detected fully opens the MOSFET, which has an extremely low forward voltage drop. When voltage is applied in the opposite direction, the substrate diode (now in reverse direction) prevents any reverse current. However, implementing this circuit requires more space on the PCB than a simple diode and the controller IC is relatively expensive.

Due to limited space on the PCB, the high-power systems, namely SEPIC and the parachute, will share a single output from the power selector to conserve space. Additionally, the SEPIC can be turned off to save energy when 5 V is not required.

The power delivery system can be seen in Figure 3.1.

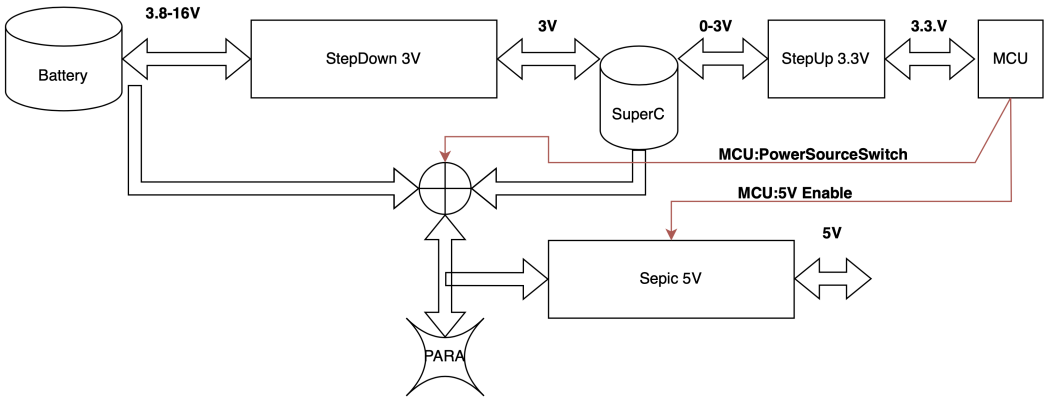

Fig. 3.1: Power delivery diagram

Considering flight dynamics, the mechanical requirements of the PCB must be taken into account. Due to the expected heavy vibrations during engine burn, the flight computer should contain as few THT (through-hole) components as possible and no mechanical moving parts except for MEMS components. During the initial high-G sequence of launch, THT parts, especially capacitors, may slightly bend and cause repeated stress on the solder, which can lead to microcracks and unwanted disconnects or voltage spikes during the launch. Additionally, THT components are often larger and heavier than SMD counterparts. To avoid such problems, electrolytic capacitors, which are both high and heavy, should not be used. Instead, tantalum and ceramic capacitors, which are lighter, smaller, and with comparable performance for the use case will be used. Moreover, any moving mechanical part during the flight would not function properly under high Gs and must not be used.

For the microprocessor, STM32WLE5JC from ST Microelectronics was chosen. SeeedStudio sells the STM32 as LoRa-E5 in a custom package, which was implemented. This choice was made based on three primary reasons: firstly, it is the same MCU used in the flight computer of the large rocket *Illustria*, thus ensuring firmware compatibility; secondly, it has a small footprint despite offering advanced features, including a significant number of GPIOs; thirdly, it has a built-in RF radio that supports the LoRa protocol at 868 MHz, which is the preferred method of communication with a ground station.

3.2 Antenna size restrictions

It is prudent to begin the design process of any wireless communication system with the component essential for its operation – an antenna. An antenna is responsible for converting electric signals in conductors to electromagnetic waves that can travel through free space. As the largest and most influential component in the wireless stack affecting the transmitted signal, its design is of utmost importance.

To achieve maximum data bandwidth and signal reception, it is critical that the main lobe of the antenna radiation pattern points in the direction "below" the rocket. This orientation guarantees optimal signal reception between the rocket and the ground station, allowing the flight computer to either use less power for transmission or transmit more data without errors.

However, achieving the desired main radiation lobe pointing downwards is a challenging task for a rocket of this size. The optimal antenna length is dependent on the wavelength λ it is designed for, and for effective transmission, a minimum practical length of an rod antenna of at least $\frac{1}{4} \cdot \lambda$ is preferable [2]. Because the planned transceiver operates at 868 MHz, the minimum practical length l can be determined using the following equation; c is the speed of light[1]:

$$\lambda = \frac{c}{f} \rightarrow l \geq \frac{c}{f} \cdot \frac{1}{4} \rightarrow l \gtrapprox 8.6\,\text{cm} \tag{3.4}$$

.

To add to the antenna complexity, the simple quarter wave monopole antenna has a radiation pattern shaped like a "donut", perpendicular to the rod [2]. Thus, it is clear that this 8.6 cm wide antenna cannot fit horizontally into the rocket's 3.5 cm wide hull and still point downwards to achieve maximum signal reception and data bandwidth.

However, there are more compact antenna designs that sacrifice efficiency for size – smaller antenna leads to worse directivity [3]. These include microstrip antennas (a trace on a PCB) [4] and dielectric antennas. The reduced efficiency of smaller antennas can negatively affect the SNR of the transmission, but because the rocket will always have a direct line of sight with a ground station, this is not a critical issue.

3.3 Antenna selection

A dipole antenna is the simplest antenna to design and build. It consists of two conductive elements, usually one-quarter a wavelength long each, separated by a gap. The elements are fed by a symmetrical current source (+ and − polarities).

[1] $c = 299,702,547\,\text{m/s}$

A monopole antenna is a type of dipole antenna that uses a ground plane as the other half of the antenna. The length of a monopole antenna is typically a quarter of the wavelength, and the body of a device/PCB can be used as the ground plane. Monopole antenna uses asymmetric feeding (Signal and Ground).

A microstrip antenna, also known as a microstrip patch antenna (MPA), is made by etching a conductive patch on a substrate and placing it next to a ground plane. The dimensions of an MPA are typically much smaller than that of a dipole or a monopole antenna. Microstrip antennas are usually used in small devices, smartphones, and IoT applications.

A dielectric antenna is a type of antenna that uses a dielectric material, such as ceramics or plastic, to radiate and receive electromagnetic waves. It might be considered as a progression of microstrip patch antennas. The dielectric has no metallic losses, unlike the MPA, which has both metallic and dielectric losses, making dielectric antennas inherently more efficient at higher frequencies, where the metallic losses are more significant [5].

The dipole antenna was chosen due to its forgiving design requirements, historical use, and easy construction. Another advantage of the dipole antenna is its ability to work effectively when its arm length is an odd multiple of half a wavelength. This feature allows for the use of the rocket's hull and fins as structural elements for the antenna, as shown in Figure 3.2. An arm length of $\frac{3}{4} \cdot \lambda \approx 25.3\,\text{cm}$ is an ideal choice for this purpose. However, the presented dipole configuration has some disadvantages, including the presence of multiple lobes, which can decrease efficiency and introduce signal strength uncertainty [6]. Additionally, the bent shape of the dipole and the metal body of the rocket engine affect the electrical conductivity and propagation of electromagnetic waves, which can impact the antenna's resonant frequency.

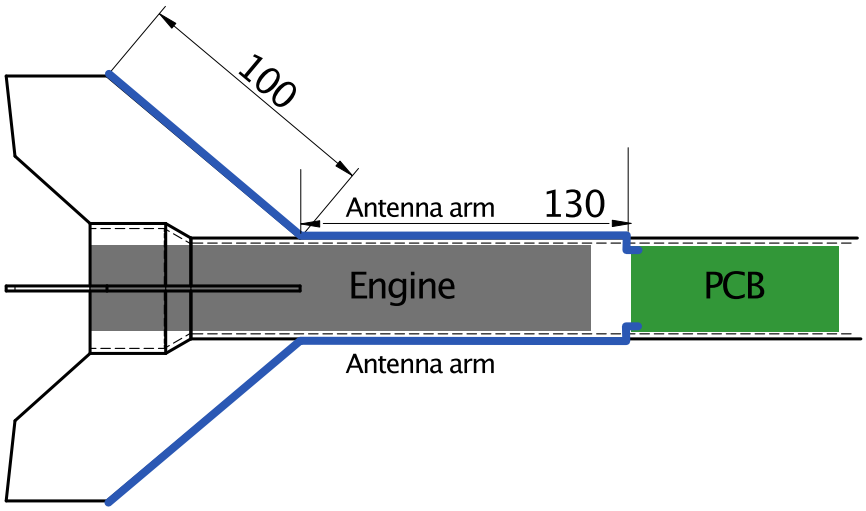

Fig. 3.2: Antenna position in the rocket; dimensions in mm

3.4 Communication protocol and LoRa

Wireless communication requires an antenna, but a functional transmission also requires the receiver and transmitter to agree on how to interpret electric signals, handle missing data, and detect errors, among other things. These communication rules are known as a protocol. The integrated LoRa protocol of the STM32 MCU is an ideal protocol to use in this case. It is important to note that only the "physical layer" of LoRa should be used, not the full LoRaWAN stack.

The LoRaWAN stack is designed for low-bandwidth communication of low-power devices over vast distances, but it cannot be used for point-to-point communication because it uses a star-of-stars topology and every packet must be received by a LoRaWAN ground station, handled by servers, and then sent to the requested device. Moreover, with a maximum packet size of between 51 and 222 bytes (depending on the spread factor), it is impossible to send sufficient data volume for meaningful monitoring [7]. The LoRaWAN architecture also has inherent delays, making it unsuitable for sending emergency abort signals or real-time telemetry transmission.

That is why usage of only the physical layer LoRa of the LoRaWAN is preferred. That way, it is possible to use the existing and tested protocol but for point-to-point real-time communication with the rocket without the restrictions imposed by LoRaWAN.

3.5 Alternative to LoRa

To address the difficulties of implementing LoRa-only communication, an alternative solution was considered. The SeeedStudio LoRa-E5 MCU comes with LoRaWAN firmware and can be used to create a new external module – a GPS module with a second LoRa-E5 to transmit the coordinates via LoRaWAN. Although this solution does not provide a continuous data stream to the base station, it solves the time-consuming problem of locating the rocket after landing. Due to limited space on the main board, the solution can only be implemented as an external board connected to the FC via SPI.

3.6 Skill evaluation and risk management

As mentioned in the requirements section, the FC holds a crucial role in the rocket's functioning. Thus, it is critical to implement measures that allow for redundancy. One such redundancy method is to integrate a standard U.FL antenna connector alongside the experimental one, with a selector in between.

Another way to future-proof the design is to expose as many of the MCU communication buses on pin headers as possible. This includes I2C, SPI, and other I/0 (Input/Output) pins from the MCU, if available. Such an array of communication methods enables the installation of pre-made 3rd party expansion boards, modules, custom boards, or quick replacement circuits if a sensor malfunctions. Examples of such boards include the GPS-LoRaWAN module mentioned earlier, 433/868 MHz transceivers, other sensors, ADC, EEPROM, and so on.

3.7 Power Distribution and Power Sources

Based on the electrical design requirements, it can be inferred that the flight computer will feature three power supplies that perform three voltage level shifts: from battery voltage to 3 V, from 3 V to 3.3 V, and from battery voltage to 5 V. In the following sections, schematic of each power supply and the key design features that will ensure optimal performance will be discussed. However, before the power supplies, let's start with the power distribution selector.

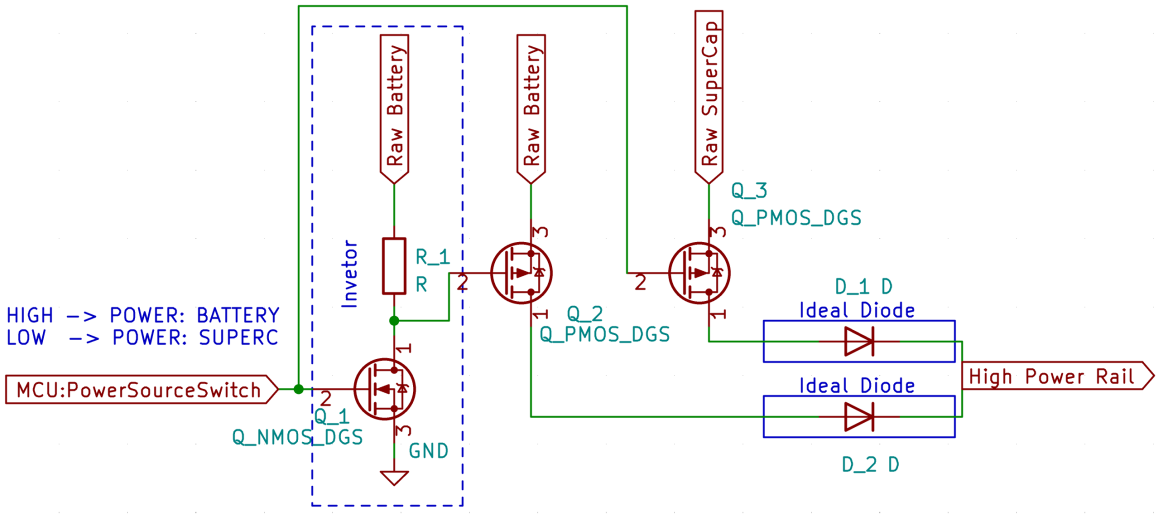

Fig. 3.3: Simplified schema of the power selector

3.8 Power Distribution Selector

The description of the power selector is limited to the selector itself, as the ideal diode principle and fundamental requirements have already been covered in Chapter *Electric Design Decisions*. To switch the power inputs, a pair of MOSFET transistors is utilized. As the transistors switch the high side of the circuit, they must be P-type to remain open when the current produces a voltage drop across the load. However, using P-type transistors creates its own set of issues. To fully close the transistor in

the chosen orientation (where the source is connected to the battery/SuperC), the gate voltage must be that of the source pin. The Gate-Source voltage poses a problem since, to save space, it is advantageous to drive the MOSFETs directly using the MCU. Unfortunately, the MCU can only supply a voltage of 3.3 V, which is significantly lower than the maximum allowed for the battery.

Taking advantage of the nature of the problem, a simple inverter can be added to the circuit by incorporating a low-current N-type MOSFET (Q_2) that can be driven by the MCU. By connecting the inverter to the battery voltage, it is possible to utilize this voltage to close the P-type MOSFET (Q_2). Figure 3.3 illustrates the inverter and the driven MOSFETs. In addition, since the SuperC has a maximum voltage of 3 V, the MOSFET (Q_3) can be turned off simply by the MCU without a level shifter. Consequently, the inverter and the gate of the Q_3 MOSFET can be linked to the same input, which will regulate both selector MOSFETs.

Figures 3.4 and 3.5 depict how the input voltage levels (HIGH and LOW, respectively) toggle between the power sources. To save space, the selector MOSFETs (Q_2 and Q_3) are integrated into a single package. The required current for the inverter MOSFETs (Q_1) is negligible, thus allowing for a small package. While a dedicated MOSFETs driver would be necessary for a quick transition between the ON-OFF states, it would take up valuable space. Nonetheless, only one transition is necessary during the flight, and the MCU can wait for a few milliseconds after switching power sources until a MOSFETs is fully open before deploying a parachute via the cutting method, which requires high current through a MOSFETs.

Since the circuit will handle high currents during parachute deployment, it is essential to minimize serial resistance and consequent heating by using traces that are as short and wide as possible. Moreover, the power selector should be positioned close to the 3 V power supply, battery, and parachute output, ideally in close proximity. However, the proximity to the SuperC is not as crucial since it will only come into play if the battery fails, and should not negatively affect the normal operation of the power selector.

3.9 3V Step-Down

The purpose of the power supply is to reduce the voltage of the battery (ranging from 3.8 V to 14.8 V) to 3 V, which will charge the SuperC and provide sufficient current to the 3.3 V power supply during regular operation. Voltage ripple does not play a significant role, as the SuperC with blocking capacitors will smooth out any ripple.

The current path for this power supply is not complicated as seen in Figure 3.6; only a few components, such as C31, D3, C32, the SW pin, D11, and L5, should be located close together. The R20 and R21 resistors serve as a voltage divider for the IC and can be placed wherever convenient. Similarly, since C35 is in parallel with the SuperC, its placement is flexible.

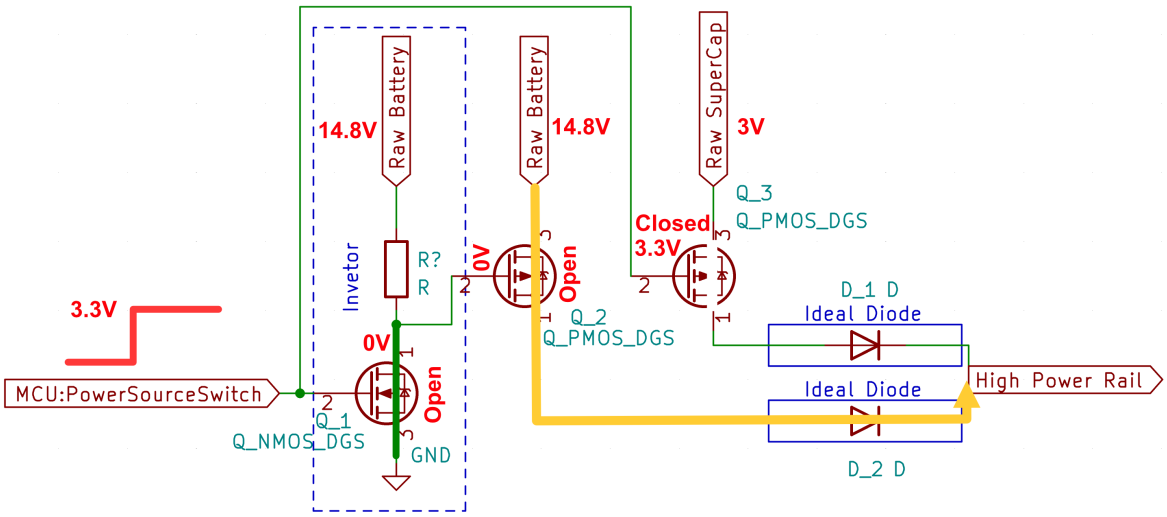

Fig. 3.4: Battery is selected when input HIGH

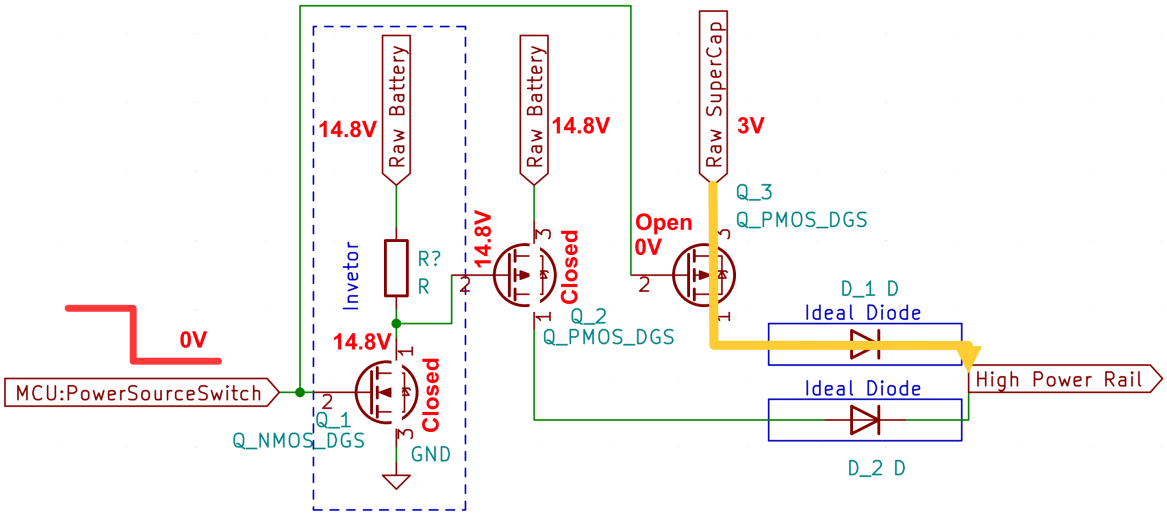

Fig. 3.5: SuperC selected when input LOW

3.10 3.3V Step-Up

To ensure proper function of the integrated circuits, including the MCU and ADC, the 3.3 V power supply should have minimal voltage ripple. This can be achieved by using output blocking capacitors and an LC filter. The use of these components results in steady voltage, and thus accurate ADC readings, and prevents voltage drops during current peaks. The power supply uses the SuperC as input, which eliminates the need for input filtering.

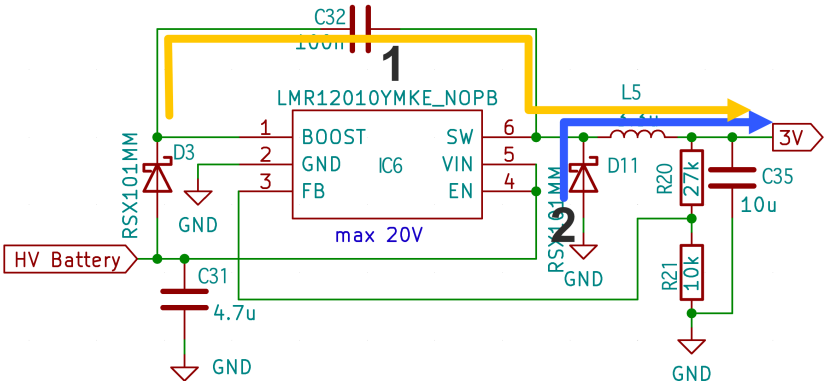

Fig. 3.6: 3V Step-Down power supply

Figure 3.7 shows that the 3.3 V power supply design has no complicated current loops. The power flows through the L4 inductor, which should be placed as close to the IC3 package (LX and BATT pins) as possible to minimize parasitic elements. A bright reader might notice that no external diode is present – it is integrated into the IC between LX and OUT pins, eliminating one component. As there is no external diode in this step-up power supply, the blocking capacitors C24 and C27 should be situated close to the OUT pin to absorb current peaks effectively. The capacitors in the filter section should be close to the inductor and other capacitors, with ground sides ideally connected.

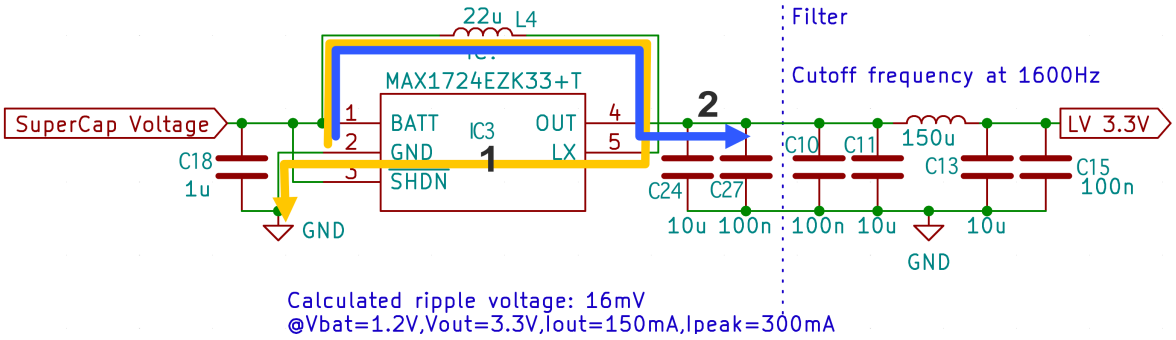

Fig. 3.7: 3.3V Step-Up power supply

3.11 5V SEPIC

The Single-ended primary-inductance converter (SEPIC) is an impressive piece of engineering that can converts input voltage to one predetermined output voltage. The input voltage can be either lower or higher than the output voltage. However, compared to "one-way" DC-DC switched power sources, it has a significantly larger footprint. To save space, instead of using two distinct inductors, a coupled one can be used [8].

The SEPIC is the most complex power supply on the board, with current loops and numerous components. As shown in Figure 3.8, during the first part of the cycle (indicated by yellow "1" arrows), when the MOSFET is open, power flows from C20+C21, through L3 and Q2, to the ground. This circuit is set to operate at a frequency of 330 kHz, so to reduce interference, the source of Q2 and the GND side of C20+C21 should ideally be in close proximity to L3. It is also beneficial to place pin no. 4 of L3 and D5 close since that is the path of the output current. Furthermore, C22 should span pins 3 and 4 of L3 and Q2 since the capacitor's polarity will switch with every cycle, resulting in high currents. The blocking capacitors at the output should be close to D5. The placement of IC4 and other not mentioned components will not significantly affect performance, and for which no strict rules are necessary.

The components' values have been calculated according to the cited application report and are available in the *Appendencies* section.

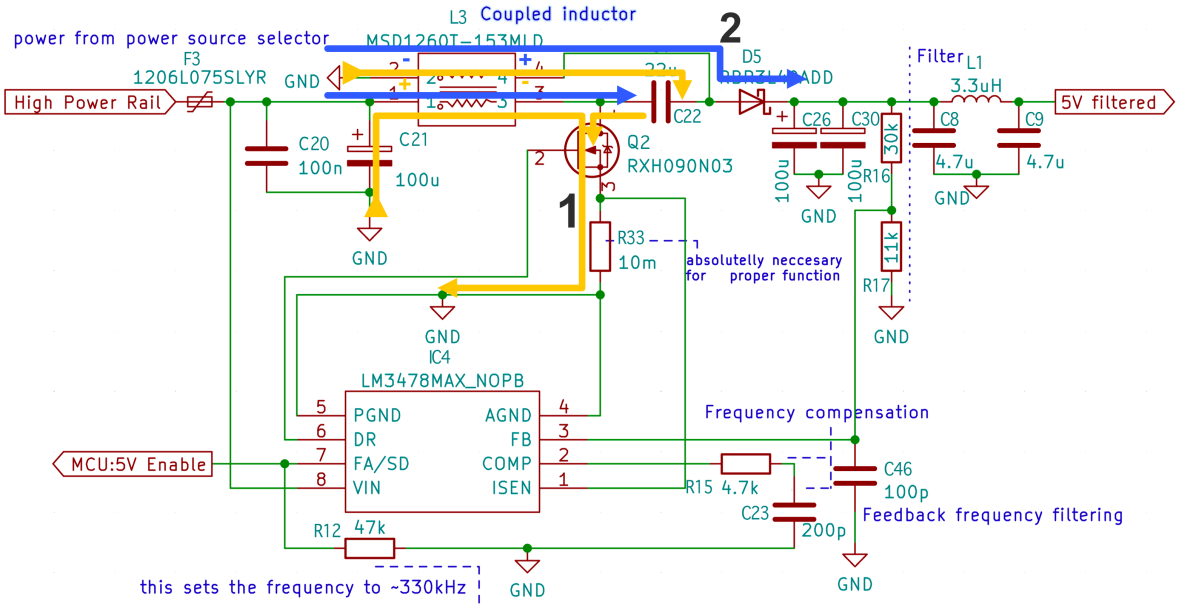

Fig. 3.8: 5V SEPIC power source

3.12 MCU Communication and programming

Communication with a PC via UART/USART is a valuable tool for programming and debugging of the MCU. Not being utilized during flight, a question arose regarding the placement of the UART<->USB translator (an FTDI chip[2]). Should it be on the main FC board, or on a separate "mother-board" that the FC connects to during programming? Despite the fact that separate boards would free up more space on the

[2]In engineering practice, this chip is commonly referred to as FTDI, after the acronym of the manufacturer

FC and reduce weight, the integrated approach was chosen for its simpler design and lower manufacturing cost compared to using two separate boards. The schema and connection to the USB connector can be seen in Figure 3.9.

To program the MCU, two SWD pins and a ground connection are used: SWDIO (data), SWCLK (clock), and GDN; which connect to a device called programmer, responsible for uploading new firmware. For programming STM32 processors, a dedicated programmer, such as the *ST-Link (V2/V3)*, can be used, or part of a *Nucleo* learning board containing a programmer. A simple 3-pin header is sufficient for connecting a programmer to the board, as the speeds are not high enough to require a special cable nor connector.

3.13 USB-C connection

For the ease of programming, the connection to the board needs to provide power and carry the necessary USB signals. After careful consideration, the USB-C connector was chosen due to its suitability for these requirements and widespread usage. The characteristics of the connector were obtained from the application note [9]. Prevalence of the USB-C standard ensures that cables are widely available and inexpensive. Additionally, the connector and cable are durable and physically reversible, allowing for easy use in either orientation.

The USB-C standard distinguishes between current sink (upstream facing port) and current source (downstream facing port) devices and can implement an active form of power delivery, which can deliver up to 5 A at 20 V (100 W) from an upstream device. However, these advanced forms of power delivery were not necessary for the current application. Without any modifications, the bare USB-C connector can provide up to 500 mA at 5 V. By adding a pair of pulldown 5.1 kΩ resistors between CC pins and GND, the device is set as a power sink and the power limit is increased to 1.5 A at 5 V, which is sufficient for measurements of power supply characteristics and normal flight computer function.

The physical connector used supports only USB 2.0 speeds, but this is not a concern as it serves only for delivering power to the board and communicating via UART, which does not require high data speed. Moreover, USB 2.0 connector comes with a smaller number of pads when compared to a USB 3.0 connector, making soldering easier. The schema of the connector and the FTDI chip can be seen in Figure 3.9.

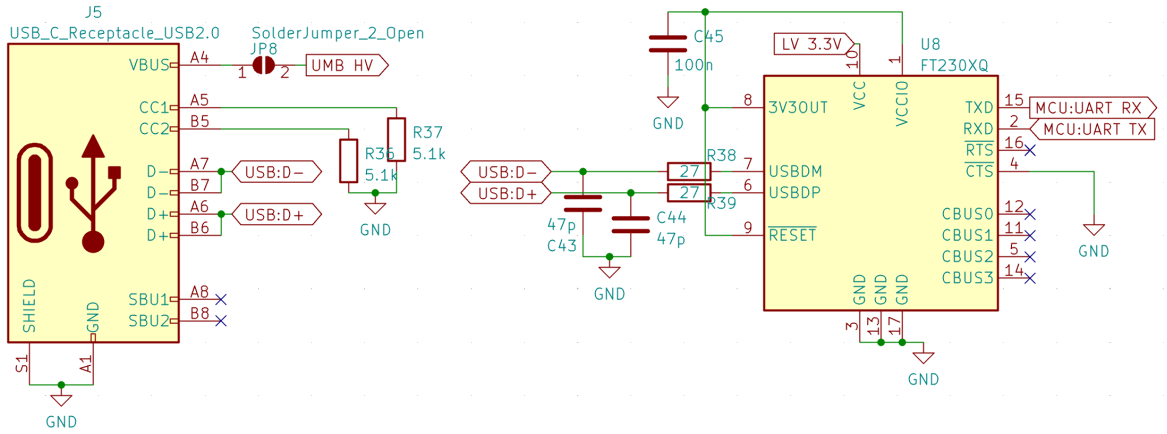

Fig. 3.9: USB-C connector with FTDI chip

3.14 Data storage

The STM32WLE5JC chip has 256 KB of flash memory to hold a program. However, since one of the key functions of the flight computer is to gather data from multiple sensors, incorporating a dedicated memory chip to store this data would prevent any memory shortages on the MCU. For this purpose, an automotive 4 MBit EEPROM memory was selected, which is a reliable type of memory commonly used in the industry. Thanks to the EEPROM technology, the data can be preserved without the need for continuous power, which is the ideal memory type for this application. The data can be stored and retrieved to and from the memory via firmware driver on the MCU.

3.15 Battery charger and battery

As the flight computer will be powered by a battery during the stand-by on the ramp and the whole flight, the issue of how to charge the battery was raised. A similar predicament as with the FTDI chip was faced: whether to integrate the charger on the board. However, it was decided that integrating a charger which would allow for charging the battery during standby would further unnecessarily complicate the PCB. Therefore, the battery must be pre-charged before placing the rocket on the launchpad. Additionally, depending on the size of the SuperC, it must be connected in advance before the flight to allow it to charge enough to start the MCU. Ideally, the battery should be charged while connected to the computer to top up the SuperC as well.

3.16 Component sizes

Choosing components with the smallest possible footprint is crucial to minimize the PCB size. The 0603[3] SMD package is the smallest package that can be placed by hand with acceptable precision. Smaller packages require a microscope for precise placement and increase the difficulty of changing them later. Hence, all low power resistors (excluding shunt resistors), blocking and low capacity capacitors were chosen in the 0603 package. For high capacity capacitors (ceramics/tantalum) and shunt resistors, 0805[4] or 1206[5] packages were preferred.

When it comes to ICs, MSOP[6] or QFP[7] packages are preferred as the leads allow for easy soldering and may serve as a makeshift measuring point, albeit with a slightly larger footprint. However, automotive or industrial grade sensors are often implemented in QFN[8] or even smaller LGA[9] packages. These no-lead packages pose soldering problems, but sensors with such qualities are often not available in MSOP or QFP packages. Having a stencil[10] made is necessary to successfully solder packages small like this.

3.17 KiCad

KiCad 6 was utilized as the primary tool in developing the project due to its comprehensive features and robust functionality. Moreover, since it is open source, no payment is required. The KiCad project with all relevant files is available in the *Appendencies*.

[3] 0603 number refers to X x Y dimensions in inches, in this case 0.06 x 0.03 in (approximately 1.55 x 0.85 mm in metric).

[4] 2 x 1.25 mm

[5] 3.2 x 1.6 mm

[6] Package with leads extending from two opposite sides of the package

[7] Package with leads extending from all four sides of the package

[8] Package without "gull wings" leads extending from four sides of the package

[9] Package with small point-like contacts on the bottom without extending leads, made for industrial soldering

[10] Stencil is a metal sheet with cutouts at the place of component's pads. After overlapping the stencil with the board, the solder can be applied only to the pads

4 Realization of the flight computer

4.1 PCB Layout

In order to ensure the best possible outcome, the schematic underwent a thorough review by multiple individuals. Following the review process, the next step was to design the printed circuit board (PCB). According to the specifications outlined in the chapter *Requirements*, the width of the PCB must not exceed 3.5 cm, and while the length can vary, shorter is preferred.

To minimize electromagnetic (EM) interference and noise induced in sensors, the logical and power supply sections were separated by a gap between the respective ground and power planes. The gap should only be bridged at the 3.3 V power supply output, as depicted in Figure 4.1, to cancel out the EM fields created by the flowing currents and minimize interference to the external circuit.

Due to the layout's density, there are two exceptions to the "section separation" rule: first, the buzzer, which is located in the 3.3 V section but powered by 5 V, has a trace that crosses the gap. To prevent current from flowing through the "3.3 V bridge" when the buzzer is active, a ground plane is positioned directly below the 5 V trace to "drain" the "introduced" current from the 5 V source. Additionally, two traces which carry only non-essential signal cross the gap at the top side of the board. These tradeoffs are acceptable, since a small voltage difference between the grounds or an increased interference when the buzzer is active, pose no significant risk to the flight computer's operation.

A unique feature of the design is the antenna section located on the right side of the PCB. The RF output pin of the MCU is linked to a selector via a 0 Ω jumper, which is positioned between the U.Fl antenna connector and a balun[1]. Traces from the balun lead to custom pads that serve as connectors for the custom-bent dipole antenna. Additional details regarding the antenna selection process can be found in the section *Antenna Selection*.

[1] component that transforms balanced signal to unbalanced and vice versa. It is used to transform the unbalanced (GND, Signal) signal from MCU to balanced (Signal +, Signal -) that the dipole antenna requires

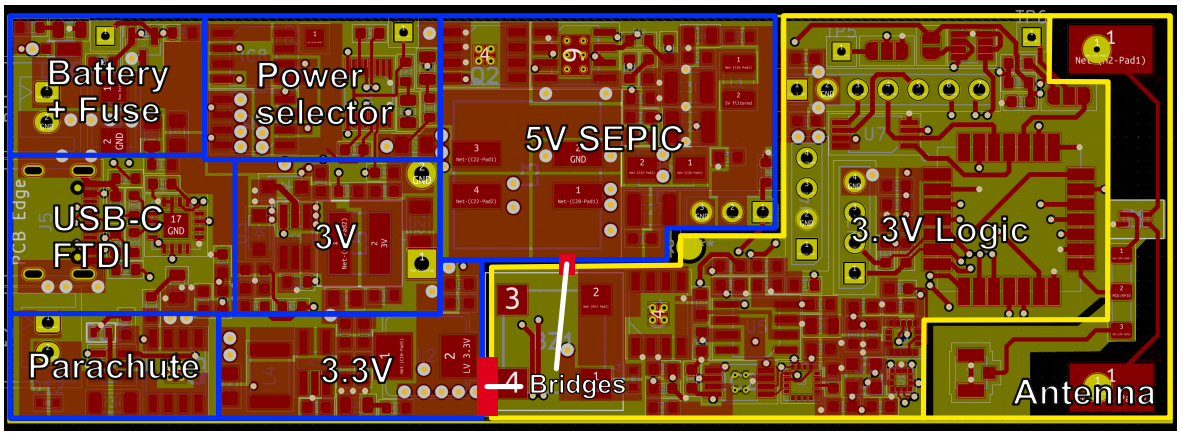

Fig. 4.1: Function-specific blocks on the PCB

4.2 Ideal diode current backflow

While designing the ideal diode, an important note in the controller datasheet must be taken into account. According to the note, "The LTC4353 can operate with input supplies down to 0 V. This requires powering the VCC pin with an early external supply in the 2.9 V to 6 V range. In this range of operation VIN should be lower than VCC. If VCC powers up after VIN and backfeeding of VCC by the internal 5 V LDO is a concern, then a series resistor (a few 100 Ω) or Schottky diode limits device power dissipation and backfeeding of a low VCC supply when any VIN is high." [10](Page 8). Simply put, if the input voltage that the controller switches is higher than the IC's power supply, current will flow in the opposite direction, from the input to the power supply. This poses a significant risk because the controller is powered by 3.3 V, and an increase in voltage in the 3.3 V rail caused by the backflow can damage the MCU, as well as other components and sensors.

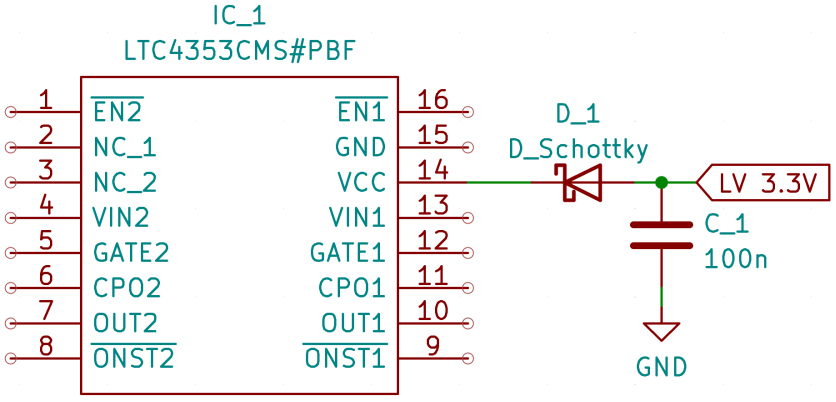

Fig. 4.2: Backflow prevention diode of Ideal Diode controller

For that reason, a backflow prevention diode was added. Schottky diode with low reverse current (500 nA) was chosen specifically to lessen the sink requirements of 3.3 V power section. An experiment confirmed that the 450 mV voltage drop across the diode does not pose significant problem to the IC while being powered by 3.3 V, although it is on the lower edge of the operating range of the IC.

4.3 PCB assembly

To aid with the solder paste application for the numerous small-size packages, a stencil was created along with the PCB. All components were then carefully placed by hand, with the exception of pin headers that had plastic spacers which would not withstand the high temperature later. The assembled board was subsequently transferred to a hot plate[2] for soldering, with the temperature gradually increased in increments of 70-100 °C until reaching 330 °C. This slow heating process was crucial in achieving optimal soldering results, as it allowed larger components to attain the necessary temperature. Hastening the temperature increase risked melting the solder before the component was adequately heated (which prevents the solder wetting the pad), leading to poor contact or even detachment of smaller components. Finally, the pin headers were soldered manually.

4.4 Power Supply Measurements

In order to evaluate the effectiveness of the power supply design, load curves were generated by measuring the output voltage of each power supply at different output currents. These results are intended to provide an overview of the behavior of the power supplies, rather than precise measurements. The measurements for the 3 V and 3.3 V supplies were taken at an input voltage of 4.2 V (measurements at 8.4 V are included in the *Appendencies*), which simulates performance with a fully charged Li-Po battery. Notably, the SuperC was *not* connected during these tests, as its presence would have likely impacted the performance of the 3.3 V power supply and also made it impossible to obtain an accurate measurement of the 3 V power supply. To conduct these measurements, a home-made variable electronic load was used, designed based on the reference design for the 36th *ZENIT v elektronike* competition [11]. However, since the device is not calibrated, the results should not be interpreted as exact.

[2]Hot plate is heating element with precise temperature control, on which a PCB can be placed. It may serve as a pre-heater (easing manual soldering) or soldering station, if the hot plate can get hot enough to melt solder.

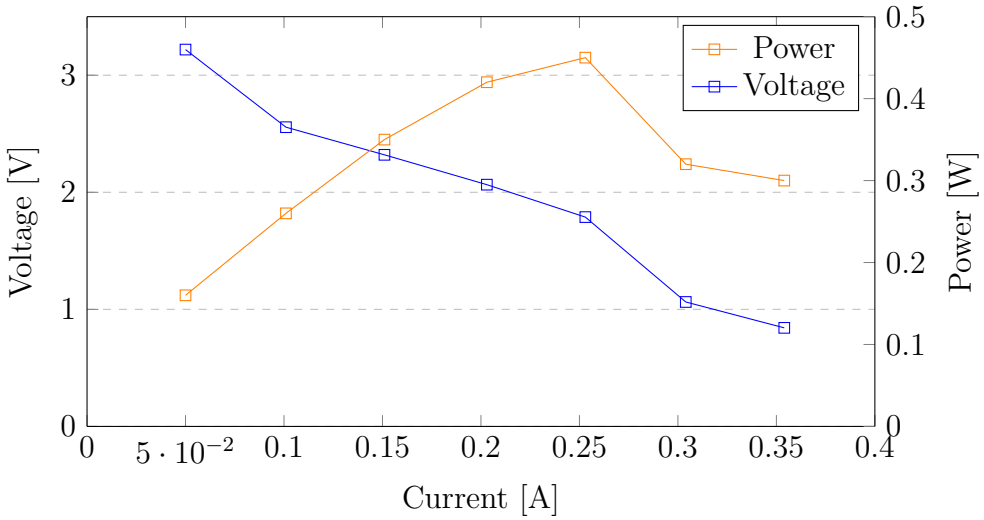

Fig. 4.3: Voltage, Power dependence of 3.3 V power supply at 4.2 V input voltage on output current

The output voltage of the 3.3 V supply falls rapidly even under light loads, as depicted in Figure 4.3. This is because the power supply IC selected has a maximum output current of only 150 mA, and the measurements were taken while the MCU, diodes, and other ICs were powered by this supply. Therefore, the graph displays the *additional* power available from the supply, up to 50 mA, above the board's current consumption without a significant voltage decrease. For power-hungry third-party modules installed on the pin header, a higher current source may be required.

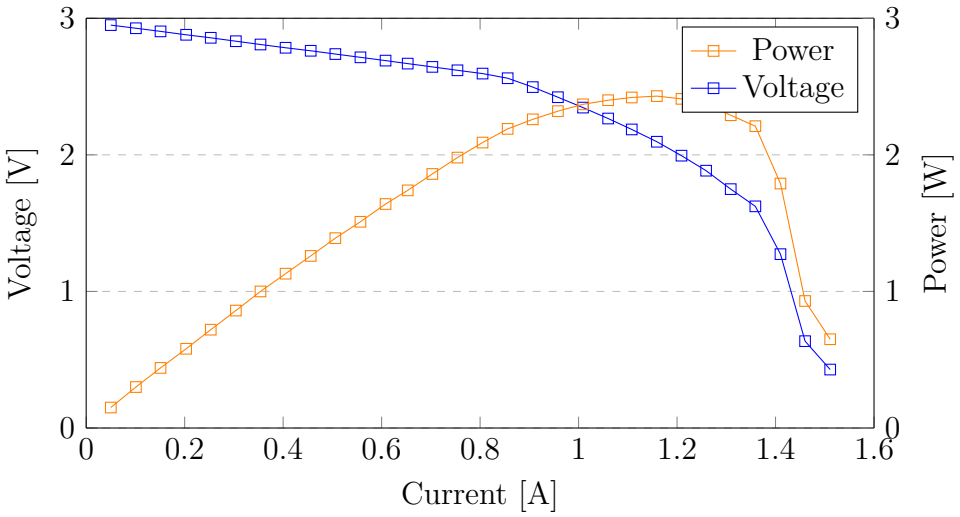

Fig. 4.4: Voltage, Power dependence of 3 V power supply at 4.2 V input voltage on output current

The 3 V power supply plays a critical role in charging the SuperC. As shown in Figure 4.4, the power supply can deliver maximum power (i.e., charging speed) to the capacitor when the output voltage is around 1.5 V. However, as the output voltage increases (i.e., as the SuperC charges), the available current gradually decreases, resulting in a slower charging rate of the SuperC as it approaches its full capacity.

In contrast to the other power supplies, the SEPIC converter was tested at three different input voltages: 3 V, 4.2 V, and 8.4 V. This was done to observe its behavior at the lowest allowed voltage (3 V) and when connected to fully charged LiPo batteries with one and two cells (4.2 V and 8.4 V, respectively).

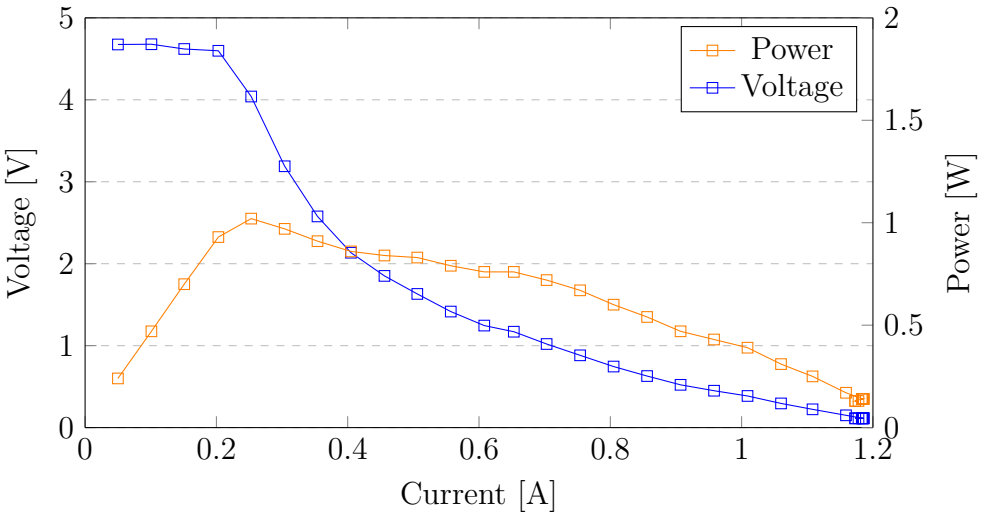

Fig. 4.5: Voltage, Power dependence of 5 V power supply at 4.2 V input voltage on output current

Upon initial inspection of Figure 4.5, it is evident that the SEPIC performs inadequately with low input voltage. However, the voltage is at the lower end of the specified operating range, which is also the voltage of the fully charged SuperC. At this voltage, the power supply can provide up to 200 mA of current without experiencing a significant voltage drop, being also the point of maximum power. However, the power output of approximately 1 W at 4 V and 200 mA is barely sufficient to operate a micro servo motor[3]. Consequently, this severely restricts the SEPIC's usefulness in the event of a main battery failure.

At nominal 4.2 V, the load curve is much closer to ideal "flat" shape, as seen in Figure 4.6. Peaking at around 5 W at 3.7 V, 1.35 A, the power is sufficient for a larger servo motor. Moreover, it can serve as a backup power output for the cutting parachute deployment method which requires high current to heat a wire.

[3]Micro servos generally require around 100 mA at 5 V for continuous rotation

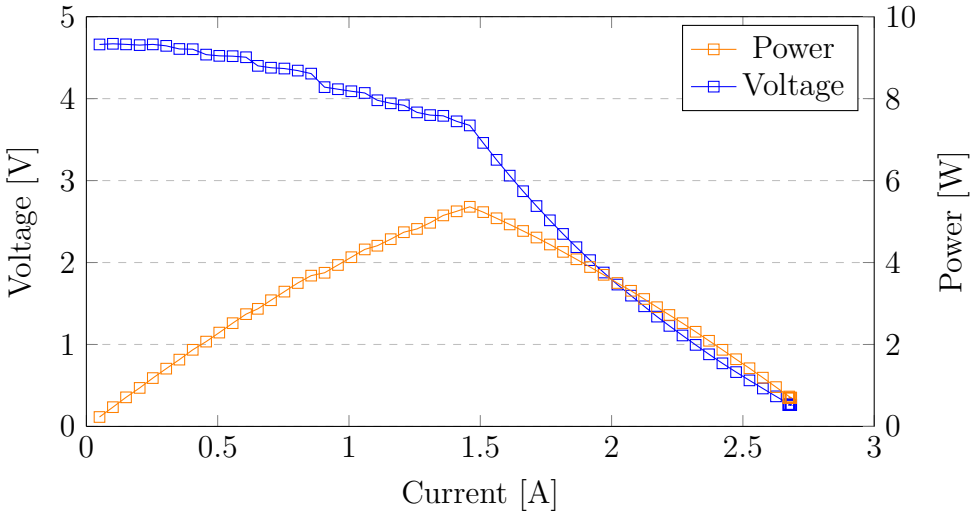

Fig. 4.6: Voltage, Power dependence of 5 V power supply at 4.2 V input voltage on output current

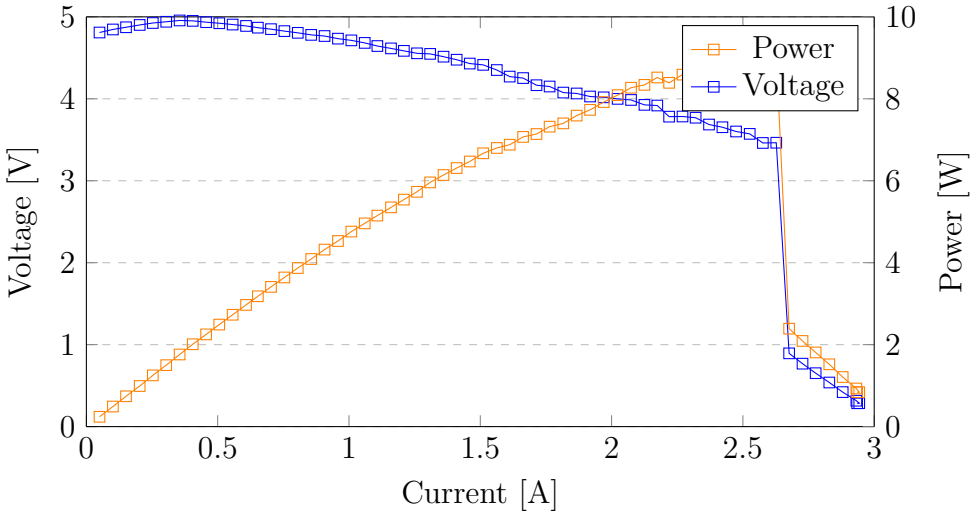

Fig. 4.7: Voltage, Power dependence of 5 V power supply at 8.4 V input voltage on output current

With an output power of nearly 9 W at 3.3 V and 2.7 A, the SEPIC's available output power is nearly proportional to the input voltage, comparing it to the previous case in which it delivered approximately 5 W at 4.2 V. This behavior is shown in Figure 4.7. Considering a minimum useful output voltage to be 4 V, at the point it can provide 8 W of power. As the output voltage is now lower than the input voltage, the SEPIC operates in step-down mode. Also, the output voltage increases slightly in the first section of the voltage curve, in contrast to the previous two measurements, in which the voltage always decreased with increased current.

Throughout all the measurements, the SEPIC exhibited a significant amount of V_{pp} values, at around 0.5-0.8 V, depending on the input voltage and load. These values indicate that the power source is not functioning properly.

The parachute deployment system, power selector, and ideal diode circuit were then measured. With the parachute output MOSFET fully open and the output short-circuited with a low-ohm resistor for high current, the voltage drop across the MOSFET was negligible. Moreover, the voltage drop across the ideal diode circuit and power selector combined was measured at 0.15 V, performing much better than a normal diode. Furthermore, the switching of power sources (battery and SuperC) was successfully tested.

Finally, the battery life of being powered only by the 70 F SuperC was measured. The capacitor was charged to full capacity at 3 V and then the external power supply was disconnected. The FC was able to run for 143.5 minutes without the battery while recording data and emitting beeps with the buzzer. This result exceeded expectations and met design requirements. However, a disadvantage of such a high capacity is the long charging time, which takes around 20-30 minutes to fully charge the capacitor and adds unnecessary mass which will not be utilized. To reduce the weight of the system during the CRC competition, a SuperC of half capacity (35 F) will be used, which is deemed adequate.

In conclusion, the performance of the power supplies is not as good as expected. The 3.3 V power supply cannot handle any more load except for a few more sensors, otherwise the voltage might drop under the lowest allowed limit of the MCU, resetting it in the process. The performance of the SEPIC at low input voltage (3 V) is underwhelming, allowing for only 200 mA of output current. At higher input voltages, the output voltage drop when loaded is still significant but should not pose problems when powering regular servo motors or external boards. On the other hand, the 3 V power supply is in a good condition, with performance as expected, since it was designed for 1A of continuous current.

4.5 StratoSat flight

The flight computer was selected as the primary computer for the *StratoSat* mission, which involved a weather balloon expedition to the stratosphere. In order to prepare for the expedition, the FC, together with a camera and it's powerbank, were placed inside a polystyrene box. A radiolocation device from CHMI was mounted outside the box, which was then attached to the balloon using a 20-meter-long string.

The requirements for the balloon expedition were quite different from those for a rocket flight. However, since the flight computer was designed to be able to adapt to a wide range of situations, it was possible to modify the computer to meet the mission's needs:

- Because the mission will fly much higher than during normal rocket launch, freezing temperatures in the upper atmosphere are dangerous for the battery. To keep the internal temperature of the electronics in acceptable levels, the power output for the parachute deployment was connected to a resistive wire as an internal heating element.
- The temperature sensor on the FC was used for monitoring the internal temperature of the electronics. Another temperature sensor for measuring the external temperature was connected to FC via I2C.
- EEPROM was used to record flight data, as intended in the original design
- The buzzer on the 5 V SEPIC was programmed to "beep" upon landing, to speed up the search for the balloon
- Pressure (and subsequent computed altitude) were measured by both internal and external sensors

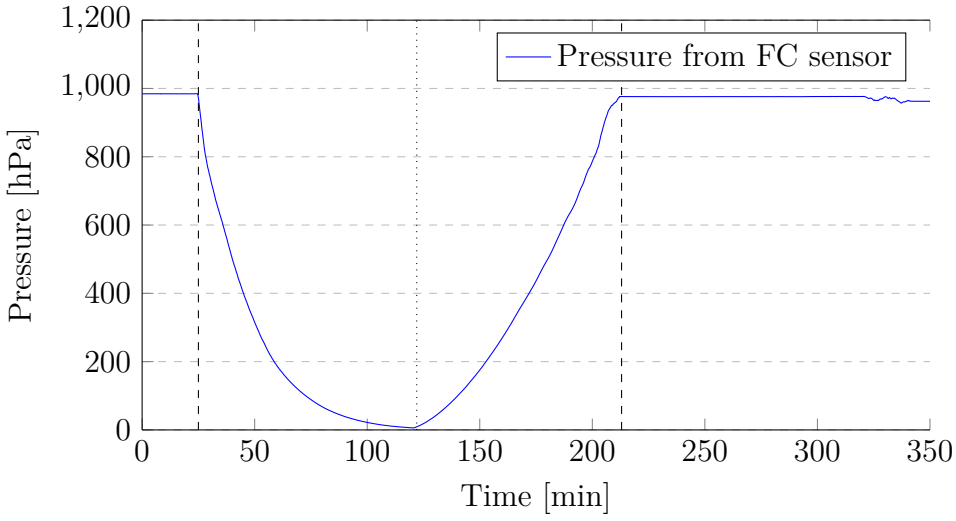

Fig. 4.8: Pressure measured by the FC sensors dependence on time from launch

The plot in Figure 4.8 reveals that the atmospheric pressure decreased to nearly 0, with a precise measurement of 592 Pa, at the highest point of the flight. This suggests that the balloon was able to attain a significant altitude. However, at such heights, the standard equation for computing altitude based on atmospheric pressure is not applicable and an equation for high-stratosphere must be used. The calculation will be described later.

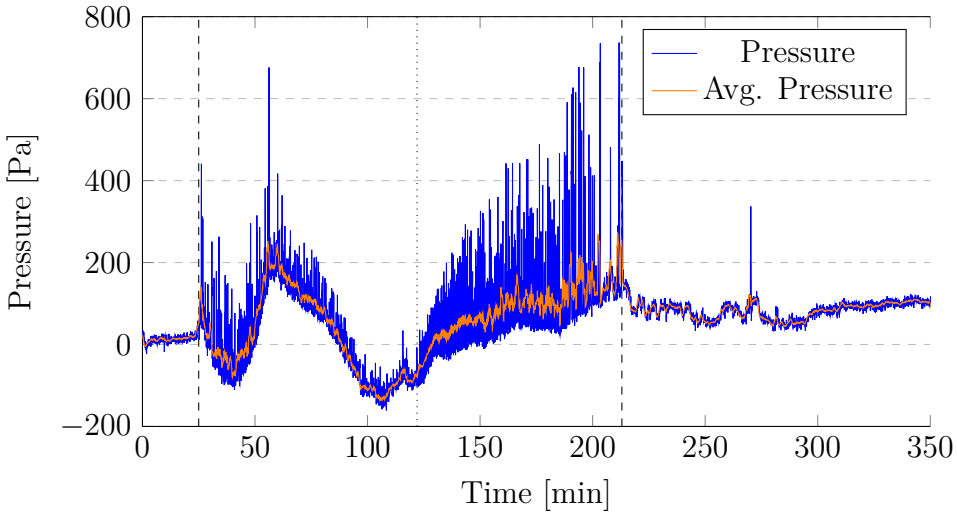

Fig. 4.9: Pressure difference of the FC and external sensors; dependence on time from launch

By comparing the data from the internal and external sensors, valuable insights can be gained. Figure 4.9 shows the difference between the pressure values measured by the two sensors. It should be noted that the external sensor was exposed to the elements as it was mounted on the side of the box. The plot reveals that the difference between the sensors is larger shortly after takeoff and before landing, forming a "V" curve with a similar shape to the pressure curve shown in Figure 4.8. The lower deviation at higher altitudes can be attributed to the overall low pressure of the surrounding air and the less turbulent conditions. The higher difference peaks before landing can be explained by wind gusts containing denser air in the lower, more turbulent parts of the troposphere. Also, it is important to note that the internal and external sensor underwent temperature changes at different rates and to a different degree, further enlarging the difference. The data was filtered using a moving average method with a time frame of 15 data points, which corresponds to a resolution of one minute[4].

It is worth comparing the magnitude of the peaks to the surrounding pressure. During the interval of the highest peaks, the surrounding pressure ranges from 700-900 kPa, which is about 100 times larger than the peaks themselves, rendering them mostly insignificant. Therefore, to better evaluate the peaks, Figure 4.10 displays the percentage of the absolute difference relative to the value measured by the FC sensor. Similar to the previous analysis, a moving average with time frame of 15 items was used. By comparing Figure 4.10 with the raw difference displayed in Figure 4.9, it can be easily observed that the point with the lowest pressure, the apogee, has the highest relative difference, thus degree having the highest degree of "uncertainty", just as expected.

[4]The data was sampled at intervals of 4.1 s, and 15 data points correspond to 61.5 s

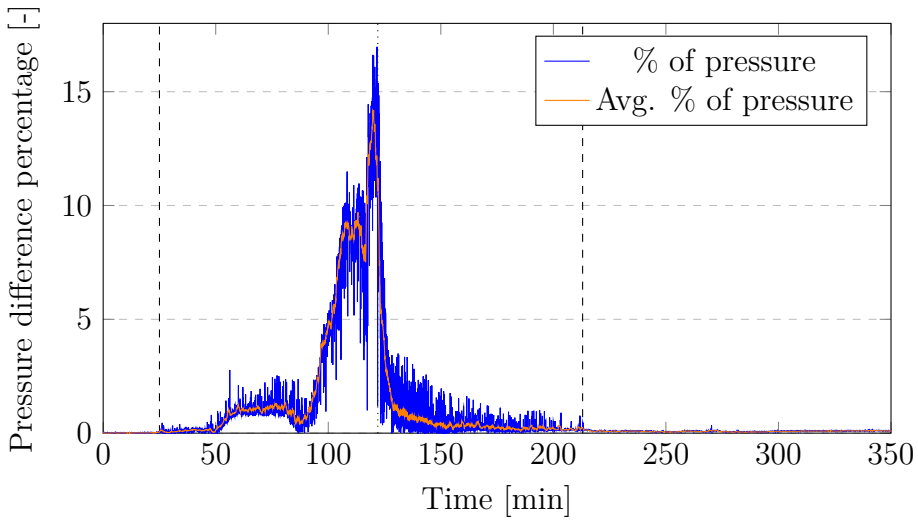

Fig. 4.10: Percentage of pressure difference between sensors and value measured by the FC

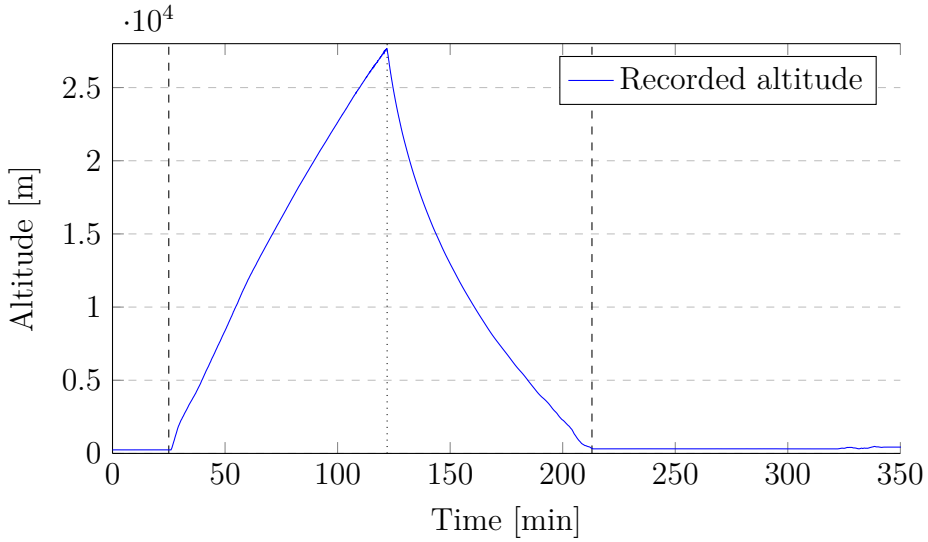

Fig. 4.11: Recorded altitude dependence on time from launch

Pressure is a parameter that can be used to calculate altitude. The pressure sensor chip used in the flight computer calculates altitude internally and sends it along with pressure data to the MCU. Figure 4.11 shows the altitude recorded by the integrated pressure sensor of the FC. However, the balloon reached an altitude higher than the end of the troposphere (11 km), which means that the internal calculation of altitude from pressure is incorrect, and a different equation must be used for the stratosphere. Additionally, the integrated pressure sensor[5] used has a minimum allowed pressure of 10 mbar (1000 Pa), which is higher than the minimum pressure recorded during

[5]MS563702BA03-50

the flight. Therefore, it is likely that the sensor output is less precise and may lead to inaccurate readings. Although the results are informative, an approximation of the altitude reached can be obtained using a set of two equations from NASA [12]. Equations 4.1 and 4.2 define the relationship between pressure p in Pa, temperature T in °C, and altitude h in meters.

$$T = -131.21 + 0.0029h \quad [°\text{C}] \tag{4.1}$$

$$p = 2488 \cdot [\frac{T + 273.1}{216.6}]^{-11.388} \quad [\text{Pa}] \tag{4.2}$$

A single equation for an altitude can be derived:

$$h = \frac{216.6 \cdot \sqrt[11.388]{\frac{2488}{p}} + 131.21 - 273.1}{0.00299} \quad [\text{m}] \tag{4.3}$$

By using the lowest measured pressure value of 592 Pa, an estimated maximum altitude of 34.8 km above sea level can be obtained through the substitution of p in Equation 4.3. However, it is important to note that this altitude should only be considered approximate, due to the pressure being outside of the range allowed by the pressure sensor's specification.

The temperature was monitored by both the FC's internal sensors and the external sensor array. In order to ensure that the batteries and other temperature-sensitive components remained within safe temperature ranges, a resistive wire was used to heat the internal electronics. This resistive wire was connected to the intended parachute deployment output and was controlled using PWM.

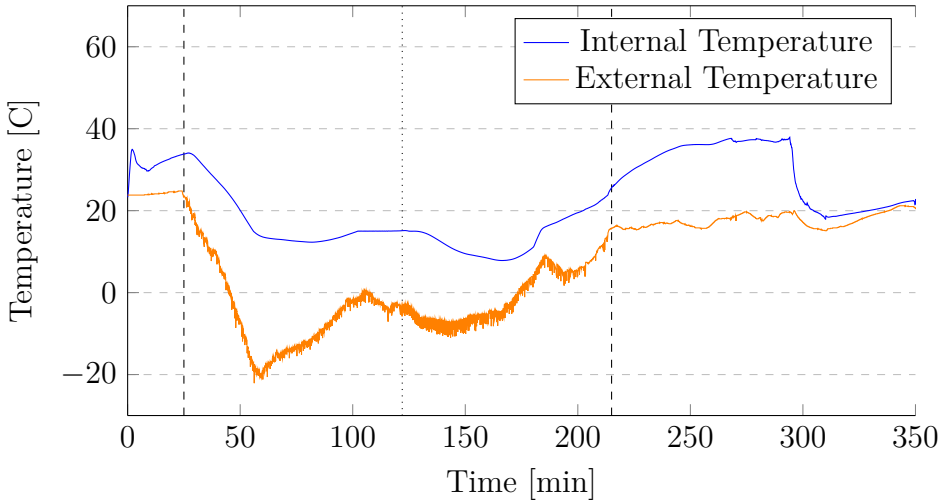

Fig. 4.12: Altitude dependence on time from launch

As shown in Figure 4.12, the minimum temperature outside the box dropped to -22.1 °C, while the internal temperature, thanks to the heating, remained above freezing, 7.83 °C at the lowest point. When compared to a standard atmospheric temperature profile, such as the one found in [13], the expected lowest temperature during an ascent through the stratosphere is around -53 °C, which is approximately 30 °C lower than what was measured. One possible explanation for this discrepancy is that the external temperature sensor was affected by the internal heating or by the sun.

4.6 LoRa

In the time of purchase, the manufacturer's firmware sets the MCU to serve as a LoRaWAN transciever. Unfortunatelly, the original firmware of the MCU cannot be retrieved or reinstalled, thus replacing it with custom code means the MCU's wireless capability must be programmed from scratch. Unfortunately, a lack of comprehensible documentation, tutorials, and examples for the STM32 MCU made the effort to get the sub-GHz RF radio to work unsuccessful. This may also be due to a lack of experience in programming STM32 MCUs. Fortunately, the design foresaw this situation, and one of the exposed buses can be used to connect an external RF radio board to the MCU.

4.7 Future Improvements

The usability of the board could be greatly improved by incorpoarating small tweaks to the schema. One potential upgrade would be the inclusion of jumpers at the power sources' outputs, allowing for testing and verification of the power supply prior to connecting it to the rest of the board. This would help to prevent component damage in the event of a faulty power supply. Additionally, a jumper at the SuperC connector could be added to allow it to be disconnected from the board.

The only area in dire need of improvement is the SEPIC. Possible solutions include recalculating component values or changing their placement to improve the SEPIC's performance. The high V_{pp} values and the output voltage waveform are particularly concerning and could potentially be addressed by changing the value of the R_{Isense} resistor, which affects the feedback loop of the SEPIC.

Finally, expertise from an individual with extensive knowledge of STM32 processors would be required to make the integrated LoRa work. If such expertise is not available, the radio section could be removed or replaced with additional sensors, measurement points, or mounting holes.

5 Results

The flight computer that was designed as the subject of this work meets all the necessary requirements for a successful rocket flight. The power selector circuit that includes the ideal diode worked flawlessly, demonstrating only a 0.15 V drop at high current loads. The supercapacitor, which was utilized as a backup power source, functioned without any problems, except for long charging times due to its 70 F capacity. This capacity proved too high, as more than 2 hours on the supercapacitor alone is unnecessary and adds needless weight. The performance of the SEPIC (Single Ended Primary Inductor Converter) was underwhelming at an input voltage of 3 V, but showed significantly improved characteristics at 4.2 V and 8.4 V. The 3.3 V power supply was selected is too weak, with only 50 mA more to source before experiencing significant voltage drop. However, the performance of the 3 V power supply was as expected. In addition, attempts to use LoRa for wireless communication were unsuccessful, necessitating the use of an external board. Finally, the functionality of the flight computer was successfully tested by a flight to 34.8 km on a weather balloon.

References

[1] Český Telekomunikační Úřad. *Všeobecné oprávnění č. VO-R/10/03.2021-4 k využívání rádiových kmitočtů a k provozování zařízení krátkého dosahu*. 2021. URL: https://www.ctu.cz/sites/default/files/obsah/vo-r10-032021-4.pdf#page=2.

[2] Thereza Macnamara. *Introduction to Antenna Placement and Installation. Aerospace Ser.* 1st ed. New York: John Wiley & Sons, Incorporated, 210. ISBN: 9780470686881. URL: https://ebookcentral.proquest.com/lib/cvut/detail.action?docID=496072.

[3] Robert C Hansen. "Fundamental limitations in antennas". In: *Proceedings of the IEEE* 69.2 (1981), pp. 170–182.

[4] Cameron Rohan, Jacques Audet, and Adrian Keating. "Small Split-Ring Resonators as Efficient Antennas for Remote LoRa IOT Systems—A Path to Reduce Physical Interference". In: *Sensors* 21.23 (2021). ISSN: 1424-8220. DOI: 10.3390/s21237779. URL: https://www.mdpi.com/1424-8220/21/23/7779.

[5] AA Kishk, KF Lee, D Kajfez, et al. "PERFORMANCE COMPARISONS BETWEEN DIELECTRIC RESONATOR ANTENNAS AND PRINTED MICROSTRIP PATCH ANTENNAS AT X-BAND." In: *Microwave Journal* 49.1 (2006).

[6] Christos G Christodoulou and Parveen F Wahid. "Fundamentals of antennas: concepts and applications". In: (2001).

[7] Ferran Adelantado et al. "Understanding the Limits of LoRaWAN". In: *IEEE Communications Magazine* 55.9 (2017), pp. 34–40. DOI: 10.1109/MCOM.2017.1600613.

[8] Dongbing Zhang. *AN-1484 Designing A SEPIC Converter*. 2001. URL: https://www.ti.com/lit/ml/snva168e/snva168e.pdf.

[9] Andrew Rogers. *Introduction to USB Type-C*. 2015. URL: https://ww1.microchip.com/downloads/en/appnotes/00001953a.pdf.

[10] Linear Technology. *LTC4353 - Dual Low Voltage Ideal Diode Controller*. 2012. URL: https://www.analog.com/media/en/technical-documentation/data-sheets/4353f.pdf.

[11] Daniel Valúch, Adam Lassak, and Martin Petrek. *Umelá záťaž s digitálnym riadením*. 2014. URL: https://dvaluch.web.cern.ch/zenit/pdf/ZENIT_2020_Zadanie_praktickej_casti.pdf.

[12] Glenn Research Center. *Earth Atmosphere Model*. 2021. URL: https://www.grc.nasa.gov/www/k-12/airplane/atmosmet.html.

[13] Edwin P. Gerber et al. *Assessing and Understanding the Impact of Stratospheric Dynamics and Variability on the Earth System*. 2014. URL: https://www.researchgate.net/figure/A-sample-vertical-temperature-profile-of-the-atmosphere-based-on-the-January_fig1_228415810.

Appendencies

Additional files provided alongside the thesis:

FlightComputerPhoto.jpg ..... Photo of the top side of the completed computer
FlightComputer.zip ..... KiCad Project containing all relevant files
Renders.zip ..... KiCad renders of the board from top and bottom
Schema.pdf ..... KiCad Schema of the final project
PowerSuppliesMeasurements.xlsx ... Excel file with power supply measurements
SEPICdesign.xlsx ..... Excel file with SEPIC component calculations